Journal of Alloys and Compounds 509 (2011) 8018–8021

Contents lists available at ScienceDirect

Journal of Alloys and Compounds

journal homepage: www.elsevier.com/locate/jallcom

# An investigation of the Al–Rh–Ru phase diagram above 50 at.% Al

B. Grushko[a,*], D. Kapush[b], T.Ya. Velikanova[b], S. Samuha[c], L. Meshi[c]

[a] PGI-5, Forschungszentrum Jülich, D-52425 Jülich, Germany
[b] I.N. Frantsevich Institute for Problems of Materials Science, 03680 Kyiv 142, Ukraine
[c] Department of Materials Engineering, Ben-Gurion University of the Negev, Beer-Sheva 84105, Israel

ARTICLE INFO

*Article history:*
Received 25 February 2011
Received in revised form 18 May 2011
Accepted 19 May 2011
Available online 27 May 2011

*Keywords:*
Aluminides
Phase diagrams

ABSTRACT

Partial 1100, 1000, 900 and 700 °C isothermal sections of the Al–Rh–Ru phase diagram were determined. The isostructural binary AlRu and AlRh phases probably form a continuous β-range of the CsCl-type solid solutions. The $Al_9Rh_2$ and C-$Al_5Rh_2$ dissolve up to 4.5 and 13 at.% Ru, while $Al_{13}Ru_4$ and $Al_2Ru$ dissolve up to 14.5 and 8 at.% Rh, respectively. A ternary orthorhombic structure (*Pbma*, $a = 2.34$, $b = 1.62$ and $c = 2.00$ nm) related to the Al–Rh ε-phases was revealed at the extension of the Al–Rh ε-phase area at compositions up to $Al_{77}Rh_{15}Ru_8$.



## 1. Introduction

The present work continues the long-term study of the alloy phase diagrams of aluminum with platinum metals (see Ref. [1] and references therein). The interest in this group of alloy systems is due to the formation of complex periodic and quasiperiodic intermetallics attractive for both basic and applied research. These binary and ternary phases are usually formed in compositional ranges between 60 and 85 at.% Al, which is also observed in binary Al–Rh [2,3] and Al–Ru [4].

The Al–Rh–Ru phase diagram has not been previously investigated. In the framework of the current study, a new orthorhombic structure (designated E) was revealed in this alloy system around the $Al_{77}Rh_{15}Ru_8$ composition. This E-phase (see Table 1 and Ref. [5] for details) was found to be structurally related to the known ε-phases in Al–Rh, Al–Pd and their ternary extensions [2,6–9].

In this contribution the phase equilibria in the Al-rich region of Al–Rh–Ru are described between 700 and 1100 °C. The phase diagrams of the binary Al–Rh and Al–Ru alloy systems are accepted according to Refs. [2,3] and Ref. [4], respectively. The data for the relevant phases from Refs. [2,4,9–17] are compiled in Table 1.

### 2. Experimental

Samples were prepared by mixing Al–Rh and Al–Ru alloys used for the determination of the corresponding binary phase diagrams published in Refs. [2,4]. The alloys were prepared by inductive melting in a water-cooled copper crucible under an Ar atmosphere, thermally annealed at 1100–700 °C for 44–352 h and subsequently water quenched.

The alloys were studied by powder X-ray diffraction (XRD, Cu Kα1 radiation was used), scanning electron microscopy (SEM) and transmission electron microscopy (TEM). The local phase compositions were determined in SEM by energy-dispersive X-ray analysis (EDX) on polished unetched cross sections. Transmission electron microscopy was carried out on a 200 kV JEOL FasTEM-2010 electron microscope equipped with an energy-dispersive X-ray spectrometer (NORAN) and Gatan slow-scan digital camera. The TEM study was preformed on powdered materials dispersed on Cu grids with amorphous carbon film. Differential thermal analysis (DTA) was carried out for selected samples at rates of 20 K/min.

## 3. Results and discussion

The binary Al–Rh and Al–Ru alloy systems contain isostructural AlRh and AlRu phases (see Table 1) which probably form a continuous β-range of the CsCl-type solid solutions. Both binary phases are congruent; therefore the Al-rich part is naturally separated from the rest of the phase diagram. At higher Al concentrations, both Al–Ru and Al–Rh exhibit cascades of peritectics from these β-phases towards (Al). The temperatures decrease sharply from 2060 °C (congruent melting of AlRh) to 655 °C (Al–Ru eutectic). The liquidus temperatures are higher at the Al–Ru than at the Al–Rh terminal.

Metallographic examinations pointed to the formation of phases along the whole 75–77 at.% Al "stripe" of the ternary phase diagram. In Al–Ru, a monoclinic M-$Al_{13}Ru_4$ phase (see Table 1) is formed inside these limits. Powder XRD and electron diffraction examinations also revealed this structure in ternary alloys containing up to at least 14.5 at.% Rh. On the other hand, in Al–Rh this Al concentration region corresponds to the ε-phases exhibiting orthorhombic symmetry. This implies a compositional discontinuity between the phase regions extending from the Al–Ru and Al–Rh terminals. The new orthorhombic structure (E-phase) mentioned in Section 1 was revealed coexisting with the ternary extension of the M-$Al_{13}Ru_4$ phase (see below). The powder diffraction patterns of both these

* Corresponding author. Tel.: +49 2461 612399; fax: +49 2461 616444.
*E-mail address:* b.grushko@fz-juelich.de (B. Grushko).

0925-8388/$ – see front matter © 2011 Elsevier B.V. All rights reserved.
doi:10.1016/j.jallcom.2011.05.074

**Table 1**
Crystallographic data of the phases mentioned in the text and isothermal sections.

| Phase | S.G. or symmetry | Lattice parameters | | | | Composition, at.% | | | Ref. |
|---|---|---|---|---|---|---|---|---|---|
| | | *a* (nm) | *b* (nm) | *c* (nm) | *β* (°) | Al | Ru | Rh | |
| $Al_9Rh_2$ | $P2_1/a$ | 0.63501 | 0.64266 | 0.87181 | 94.809 | 81.8 | – | 18.2 | [10] |
| $\varepsilon_6$[a] | *Pnma* | 2.34 | 1.65 | 1.24 | – | 75.0 | – | 25.0 | [2] |
| $\varepsilon_{16}$[a] | *B2mm* | 2.38 | 1.64 | 3.28 | – | 76.0 | – | 24.0 | [2,9] |
| C-$Al_5Rh_2$ | $Pm\bar{3}$ | 0.7680 | – | – | – | 72.0 | – | 28.0 | [11,12] |
| | | 0.77163(3) | – | – | – | 74.2 | 12.5 | 13.3 | This work |
| H-$Al_5Rh_2$ | $P6_3/mmc$ | 0.7905 | – | 0.7861 | – | 71.0 | – | 29.0 | [12,13] |
| V-$Al_7Rh_3$ | *Monocl.* | 1.0309 | 0.3808 | 0.6595 | 102.42 | 70.0 | – | 30.0 | [12] |
| AlRh AlRu (β) | $Pm\bar{3}m$ | 0.280 | – | – | – | ~50.0 | – | ~50.0 | [14] |
| | | 0.295 | – | – | – | ~50.0 | ~50.0 | – | [15] |
| | | 0.29717(19) | – | – | – | 54.5 | 13.5 | 32.0 | This work |
| $Al_3Ru_2$ | *I4/mmm* | 0.3079 | – | 1.433 | – | 60.0 | 40.0 | – | [15] |
| $Al_2Ru$ | *Fddd* | 0.8012 | 0.4717 | 0.8785 | – | 66.7 | 33.3 | – | [15] |
| $Al_5Ru_2$ | *Cmcm* | 0.78[a] | 0.66[a] | 0.42[a] | – | 71.4 | 28.6 | – | [4] |
| $Al_{13}Ru_4$ | *C2/m* | 1.5862 | 0.8188 | 1.2736 | 107.778 | 76.5 | 23.5 | 14.0 | [16] |
| | | 1.5647(5) | 0.8274(3) | 1.2651(4) | 107.82(3) | 76.0 | 10.0 | | This work |
| $Al_6Ru$ | *Cmcm* | 0.74882 | 0.65559 | 0.89605 | – | 85.7 | 14.3 | – | [17] |
| E[a] | *Pbma* | 2.34 | 1.62 | 2.00 | – | 77.0 | 8.0 | 15.0 | [5] |

[a] Electron diffraction data.

phases are shown in Fig. 1. The E-phase is formed at the extension of the *ε*-region. No reliable compositional discontinuity was observed between the E phase and the binary *ε*-phase region by either of the applied methods.

Extensive TEM examinations of the samples with 4 or 5 at.% Ru (i.e. somewhat lower Ru concentration than of the above-mentioned E-phase) usually revealed decagonal-like patterns, i.e. an overall tenfold symmetry (see Fig. 2) and only definite periodicity of ~1.62 nm in a perpendicular direction. In spite of some similarity to a decagonal $D_4$-phase, they probably belong to the same E-phase, whose small domains are only oriented along the *b*-axis. Indeed, several reflections are definitely split or exhibit a triangle spot shape (shown by arrows in Fig. 2). This can be illustrated by the similarity of the powder XRD patterns taken from the samples whose TEM examinations revealed either the E-phase or the decagonal-like patterns. A typical region of such a pattern is shown in Fig. 3a in comparison with that of the stable $D_4$-phase in the

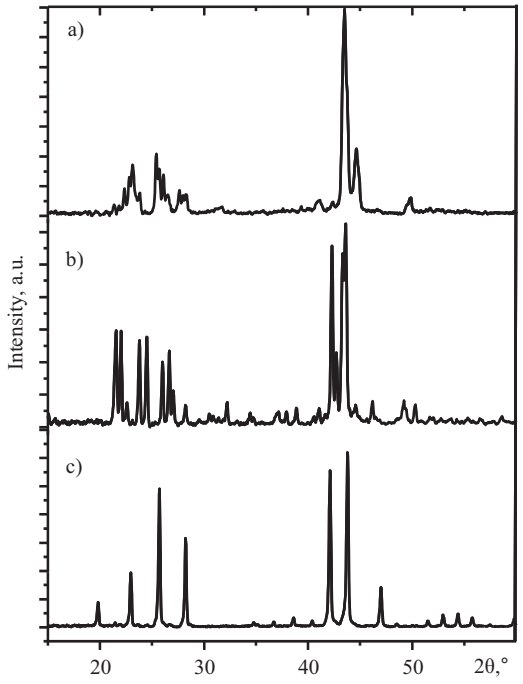


**Fig. 1.** Powder XRD patterns (Cu Kα1 rad.) of the (a) E-phase, (b) M-$Al_{13}Ru_4$ phase containing 14 at.% Rh and (c) C-phase containing 13 at.% Ru.

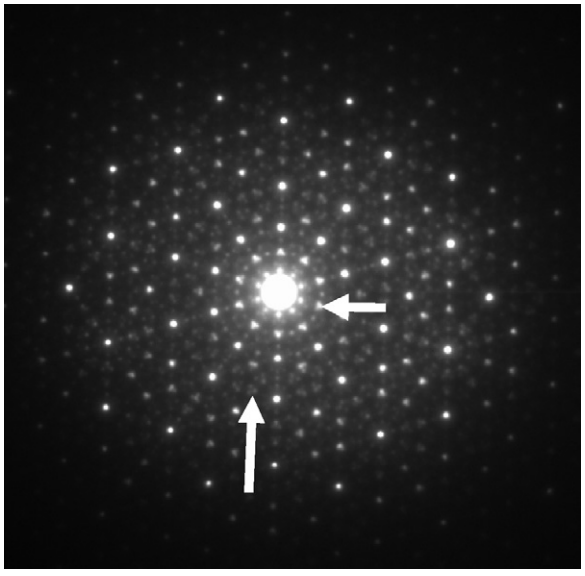

**Fig. 2.** Electron diffraction pattern exhibiting pseudo-decagonal symmetry. The "triangle" spots and splitting of reflections are marked.

Al–Ni–Ru alloy system (Fig. 3b, from Ref. [18]). The pattern in Fig. 3a contains split reflections around the positions of the reflections of the true decagonal phase.

It is plausible to suggest that the overall decagonal-like symmetry observed in the electron diffraction patterns follows from the symmetry of the solidified material which could contain a metastable decagonal phase. Small domains of the E-phase formed by annealing could inherit the overall symmetry. Such a transition was studied in more detail in the Al–Pd–Fe alloy system in Ref. [19]. In the latter case, the resulting structure belonged to the *ε*-family. A close structural relation of the E-phase to the *ε*-family is demonstrated in Ref. [5]. Therefore, we cannot exclude that some decagonal-like patterns observed in the present work could also belong to the *ε*-phases. This is an additional obstacle in the experimental specification of the compositional regions belonging to E and *ε*-s.

In the Al–Rh phase diagrams presented in Refs. [2,3] the $\varepsilon_{16}$ and $\varepsilon_6$ structures[1] correspond to two phases separated by a two-phase

[1] In Refs. [2,3] they are designated $O_1$ and $O_2$, respectively.

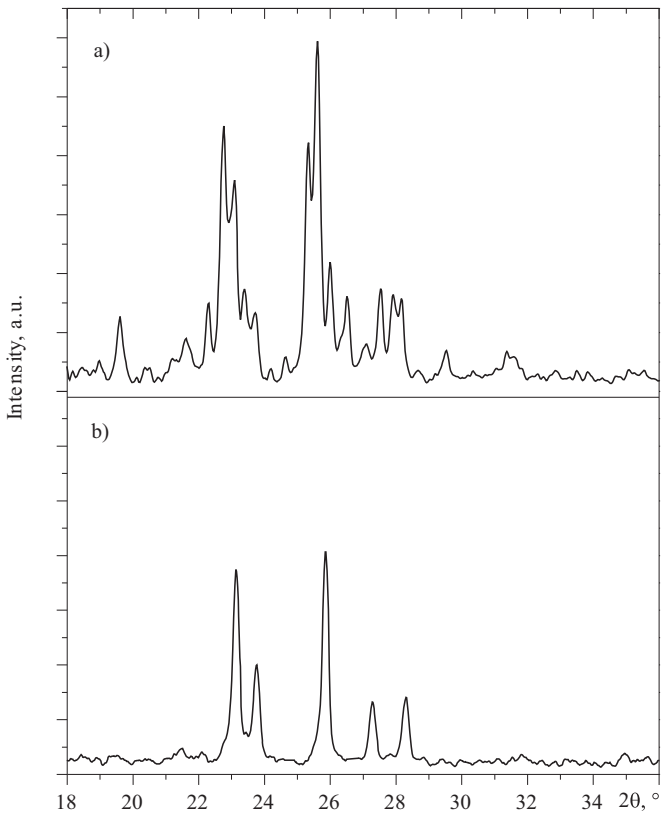


**Fig. 3.** Powder XRD pattern (Cu Kα1 rad.) of the sample where the pseudo-decagonal electron diffraction patterns in Fig. 1 was taken from (a) in comparison with that of the Al–Pd–Ru $D_4$ decagonal phase (b).

region and melting at different temperatures. However, this two-phase region was not observed experimentally and the published phase diagrams were estimated considering the very weak thermal effects associated in Refs. [2,3] with reactions involving two neighboring ε-phases. This is a similar situation in Al–Pd exhibiting the formation of $\varepsilon_6$ and $\varepsilon_{28}$ [6]. More extensive investigation of a number of ternary systems based on Al–Pd and Al–Rh (see Ref. [1] and references therein) revealed continuous ε-regions extending far into ternary compositions and exhibiting different structural variants of ε, both regular and aperiodic in the *c*-direction. Moreover, the geometric description of the "higher-order" ε-phases shows their formation from the "basic" $\varepsilon_6$ structure via ordering of specific defects (see in Ref. [8] and references therein). This is in favor of the compositional continuity of the ε-regions, which is most probably also typical of the binary Al–Rh and Al–Pd systems, where the experimental clarification of the continuity is difficult due to very narrow compositional regions.

On the other hand, the E-phase is built from τ-times larger "clusters" and its tiling elements cannot be obtained from those of the ε-family by the introduction of similar defects [5]. Therefore, this is not in favor of the continuity of the E and ε regions. However, the implied E–ε two-phase region could be very narrow. In the isothermal sections in Fig. 4 these regions are conditionally combined (also see below for a comparison with Al–Pd–Ru).

The high-temperature Al–Rh C-phase (see powder XRD in Fig. 1c) forming at slightly lower Al concentrations also extends far into ternary compositions at practically constant Al.

Due to the much higher melting temperatures of the lower-Al phases the region between the β-phase and the M–ε compositional line was only studied at 1000 and 1100 °C.

The results concerning the equilibria at 1100 °C (Fig. 4a) and 1000 °C (Fig. 4b) are quite similar. The maximal solubility of Al

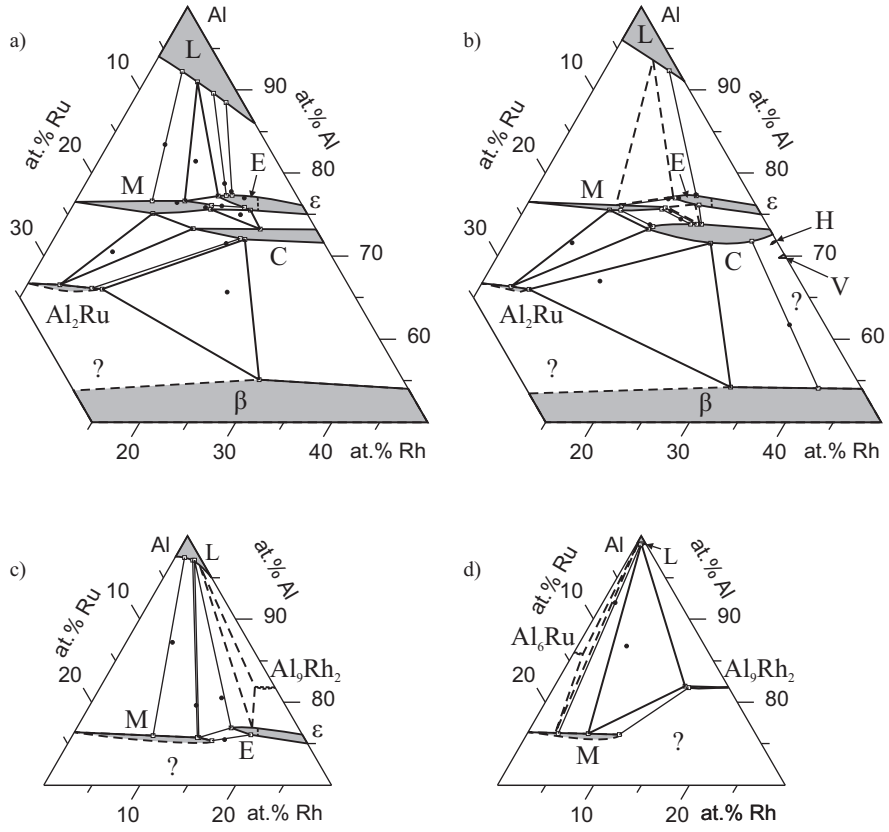


**Fig. 4.** Phase equilibria in the Al-rich part of Al–Rh–Ru at (a) 1100 °C, (b) 1000 °C, (c) 900 °C and (d) 700 °C. The liquid is designated L. The compositions of the studied alloys are marked by spots. The compositions of the phases determined by SEM/EDX are shown by squares. Provisional tie-lines are shown by broken lines.

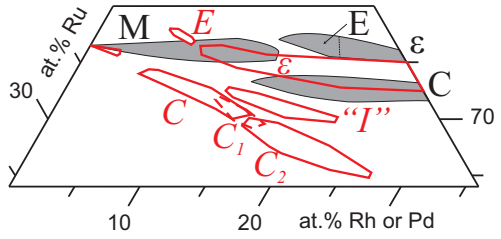


**Fig. 5.** Comparison of the compositional regions of M, ε, C phases in Al–Rh–Ru (black lines, filled) and Al–Pd–Ru (red) determined in Ref. [20]. (For interpretation of the references to color in this figure legend, the reader is referred to the web version of this article.)

in the β-phase reaches 55 at.%. Of the Al–Ru phases, $Al_2Ru$ was found to dissolve up to 8 at.% Rh and M-$Al_{13}Ru_4$ up to 14.5 at.% Rh extending at almost constant Al concentrations. The $Al_5Ru_2$ phase, existing at temperatures much higher than the annealing temperatures, was only observed in solidified material. It contained up to 7 at.% Rh. The solubility of Rh in $Al_3Ru_2$ was not studied. Of the Al–Rh phases, high-temperature cubic C-$Al_5Rh_2$ phase was found to extend up to 13 at.% Ru. The total region of the E and ε-phases extends up to ~8 at.% Ru. The Ru solubility in the low-temperature hexagonal H-$Al_5Rh_2$ phase and the monoclinic V-phase is below the values limited by the C–β tie-line in Fig. 4b. The region between this tie-line and the Al–Rh terminal was not studied in more detail.

At 900 °C (Fig. 4c) the binary monoclinic $Al_9Rh_2$ is already solid but its propagation to the ternary space up to 4.5 at.% Ru was only experimentally observed at 700 °C (Fig. 4d). At the latter temperature only the three-phase equilibrium M-$Al_9Rh_2$–L was achieved for reasonable times. The solubility of Rh in $Al_6Ru$ is less than 2 at.% (limited by the M–L tie-line in Fig. 4d).

## 4. Comparison with Al–Pd–Ru

Apart from Al–Rh the ε-phases are also formed in Al–Pd [6]. Therefore it is interesting to compare the present results with those obtained in Ref. [20] for the Al–Pd–Ru alloy system. The compositional regions of the relevant Al–Rh–Ru and Al–Pd–Ru phases are overlapped in Fig. 5. The overall compositional region of the Al–Pd ε-phase(s) is completed in accordance with the binary phase diagram up to ~75 at.% Al. It is somewhat shifted towards lower Al concentrations with respect to that in Al–Rh, but the compositions of $\varepsilon_6$ are in agreement in both binary systems. In contrast to Al–Rh, the $\varepsilon_{16}$ structure was not observed in Al–Pd but together with $\varepsilon_6$, typical of both the binary systems, $\varepsilon_{28}$ was found to form in Al–Pd at lower Al concentrations [6].[2]

The ternary extension of the ε-phases in Al–Pd–Ru is significantly wider than in Al–Rh–Ru. Increasing Ru concentration results in an increase of the Al limit of the ε-phase(s) achieving those in Al–Rh, thus at the high-Ru limit of the ε-region the $\varepsilon_{16}$-structure, typical of Al–Rh, is formed. In both ternary alloy systems compared here the orthorhombic E-phases related to ε–s were revealed close to the high-Ru end of the ε-regions. Although in Al–Pd–Ru no single orientation of the E-phase was found, the lattice images observed in both systems were locally identical [5]. On the other hand, a separation of the E and ε regions only suggested in Al–Rh–Ru was observed in Al–Pd–Ru [20].

In contrast, the solubility of Pd in the M-$Al_{13}Ru_4$ phase is significantly lower than that of Rh. It is worth noting that a monoclinic phase isostructural to M-$Al_{13}Ru_4$ is formed in Al–Co (see Ref. [21] and references therein, Co and Rh belong to the same column of the periodic table). Therefore it might also be possible to form such a structure as a metastable phase in Al–Rh, but less plausibly in Al–Pd. Wider extension of the M-region in Al–Rh–Ru is in favor of such a suggestion.

No phase isostructural to C-$Al_5Rh_2$ is stable in Al–Pd but such a structure was revealed in Al–Pd–Ru. This ternary C-phase is formed at Al concentrations similar to those for C-$Al_5Rh_2$ (see Fig. 5). Two related structures $C_1$ and $C_2$ are formed in Al–Pd–Ru at lower Al concentrations [20]. They were not observed in binary Al–Pd, Al–Ru and ternary Al–Rh–Ru systems. Similarly, neither the icosahedral phase nor the three related cubic structures forming in Al–Pd–Ru in the region designated "I" [20] was observed in the Al–Rh–Ru system.

## 5. Conclusions

In conclusion, partial isothermal sections of Al–Rh–Ru were determined at 1100, 1000, 900 and 700 °C. The $Al_9Rh_2$ and C-$Al_5Rh_2$ dissolve up to 4.5 and 13 at.% Ru, while $Al_{13}Ru_4$ and $Al_2Ru$ dissolve up to 14.5 and 8 at.% Rh, respectively. A new ternary intermetallic E-phase (*Pbma*, $a = 2.34$, $b = 1.62$ and $c = 2.00$ nm) was revealed at the extension of the Al–Rh ε-phase area at compositions of up to $Al_{77}Rh_{15}Ru_8$.

## Acknowledgements

We thank V. Ezersky, A. Besmehn and C. Thomas for technical assistance and D. Pavlyuchkov for helpful discussions. D.K. thanks Forschungszentrum Jülich for financial support and hospitality.

## References

[1] B. Grushko, T.Ya. Velikanova, CALPHAD 31 (2007) 217.
[2] B. Grushko, J. Gwóźdź, M. Yurechko, J. Alloys Compd. 305 (2000) 219.
[3] V.G. Khoruzhaya, K. Korniyenko, P.S. Martsenyuk, T.Ya. Velikanova, Powder Metall. Met. Ceram. 45 (5–6) (2006) 251.
[4] S. Mi, S. Balanetskyy, B. Grushko, Intermetallics 11 (2003) 643.
[5] L. Meshi, S. Samuha, D. Kapush, D. Pavlyuchkov, B. Grushko, J. Alloys Compd. 509 (2011) 6551.
[6] M. Yurechko, A. Fattah, T. Velikanova, B. Grushko, J. Alloys Compd. 329 (2001) 173.
[7] H. Klein, M. Audier, M. Boudard, M. de Boissieu, L. Beraha, M. Duneau, Philos. Mag. A73 (1996) 309.
[8] S. Balanetskyy, B. Grushko, T.Ya. Velikanova, Z. Kristallogr. 219 (2004) 548.
[9] M.G. Li, J.L. Sun, P. Oleynikov, S. Hovmöller, X.D. Zou, B. Grushko, Acta Crystallogr. B66 (2010) 17.
[10] M. Boström, H. Rosner, Yu. Protz, U. Burkhard, Yu. Grin, Z. Anorg. Allg. Chem. 631 (2005) 534.
[11] Yu. Grin, K. Peters, U. Burkhardt, K. Gotzmann, M. Ellner, Z. Kristallogr. 212 (1997) 439.
[12] B. Grushko, M. Yurechko, Z. Kristallogr. 214 (1999) 313.
[13] L.E. Edshammar, Acta Chem. Scand. 21 (1967) 647.
[14] T. Shishido, H. Takei, J. Less-Common Met. 119 (1986) 75.
[15] L.E. Edshammar, Acta Chem. Scand. 20 (1966) 427.
[16] L.E. Edshammar, Acta Chem. Scand. 19 (1965) 2124.
[17] L.E. Edshammar, Acta Chem. Scand. 22 (1968) 2374.
[18] S. Mi, B. Grushko, C. Dong, K. Urban, J. Alloys Compd. 359 (2003) 193.
[19] S. Balanetskyy, B. Grushko, T.Ya. Velikanova, K. Urban, Intermetallics 13 (2005) 649.
[20] D. Pavlyuchkov, B. Grushko, T.Ya. Velikanova, J. Alloys Compd. 469 (2009) 146.
[21] B. Grushko, R. Wittenberg, K. Bickmann, C. Freiburg, J. Alloys Compd. 233 (1996) 279.

[2] More recent investigations (unpublished) indicated the formation of $\varepsilon_6$ at lower temperatures also at the low-Al limit of the binary ε-region, while $\varepsilon_{28}$ was observed in samples annealed at higher temperatures.